2021

# Corrosion failure of titanium tubes of a heat exchanger for the heating of dissolving lye

Valentin Romanovski

Yolanda S. Hedberg

Andrei Paspelau

Vitali Frantskevich

James J. Noël

*See next page for additional authors*

## Authors

Valentin Romanovski, Yolanda S. Hedberg, Andrei Paspelau, Vitali Frantskevich, James J. Noël, and Elena Romanovskaia

# Corrosion Failure of Titanium Tubes of a Heat Exchanger for the Heating of Dissolving Lye

**Valentin Romanovski[1,2,*], Yolanda S. Hedberg[3,4], Andrei Paspelau[5], Vitali Frantskevich[5], James J. Noël[3,4], Elena Romanovskaia[6,*]**

[1] Science and Research Centre of Functional Nano-Ceramics, National University of Science and Technology "MISIS", 119049, Lenin av., 4, Moscow, Russia
[2] Institute of General and Inorganic Chemistry, National Academy of Sciences of Belarus, 220072, Surganova st., 9/1, Minsk, Belarus
[3] Department of Chemistry, The University of Western Ontario, London, Ontario, N6A 5B7, Canada
[4] Surface Science Western, The University of Western Ontario, London, Ontario, N6G 0J3, Canada
[5] Belarusian State Technological University, 220006, Sverdlova st., 13, Minsk, Belarus
[6] Department of Materials Science and Engineering, University of Virginia, Charlottesville, VA, 22904, USA

* Corresponding author: vramano@kth.se; Lenin av., 4, Moscow, Russia, 119049; Elena Romanovskaia, ggd2dr@virginia.edu; Charlottesville, VA, 22904, USA

**Running title:** Titanium corrosion during sylvinite ore processing

**ORCID:**
**Valentin Romanovski:** 0000-0003-1741-0316
**Yolanda Hedberg:** 0000-0003-2145-3650
**James J. Noël:** 0000-0003-3467-4778
**Elena Romanovskaia:** 0000-0001-8815-356X

**Abstract**
Corrosion of titanium heat exchangers in the processing of sylvinite ore is undesirable from economic, safety, and process sustainability perspectives. Triggered by an industrial case, we investigated the extent of corrosion during simulated contact with sylvinite ore (in dissolving lye) in relevant conditions. Detailed characterization of the failed tubes and corrosion products was carried out to understand the mechanism of failure. Corrosion of titanium (Grade 2) tubes was investigated at room temperature, 60, 70, 80, and 90 °C. After electrochemical and surface morphology analysis, we found that pitting corrosion of the titanium tube material sharply increased above 80 °C in the simulated sylvinite ore environment (pH 7.1). The failure analysis revealed extensive degradation by transgranular cracking through both the oxide and metal matrix, likely caused by a combination of the high temperature, pressure, possible vibrations, the build-up of lye deposits causing crevices, the high salt content of the lye, and possibly metal (copper, iron, zinc) impurities/deposits in or on the titanium metal, which can catalyze hydrogen evolution.

**Key words:** titanium; corrosion; heat-exchanger; chlorine; sylvinite ore; cracking

**Data Availability**
Some or all data, models, or code that support the findings of this study are available from the corresponding author upon reasonable request.

**CRediT authorship contribution statement**
**Valentin Romanovski:** Supervising, Conceptualization, Methodology, Investigation, Data curation, Formal analysis, Visualization, Writing – original draft, Writing – review & editing. **Yolanda Hedberg:** Data curation, Formal analysis, Writing – original draft, Writing – review & editing. **Andrei Paspelau:** Investigation. **Vitali Frantskevich:** Formal analysis. **James J. Noël:** Data curation, Formal analysis, Writing – original draft, Writing – review & editing. **Elena Romanovskaia** Investigation, Data curation, Formal analysis.

**Competing Interests:** Authors declare no competing interests.

## Introduction

Titanium metal and alloys are widely used in chemical processing industries for applications in any aggressive media because of their high corrosion resistance [1]. At the same time, titanium is very sensitive to certain environmental conditions. For example, titanium equipment can fail due to exposure to hydrogen leading to hydrogen embrittlement [2, 3]. The presence of iron (Fe) can serve as a catalyst for the evolution of hydrogen [4]. Also, abrasive wear is a common cause of failure [5–8]. Previously, titanium heat exchanger tubes failed due to fatigue [9] and even due to fluid-induced vibrations [10].

A titanium condenser tube with seawater at the tube side and hydrocarbon (low-pressure steam) at the shell side was found to fail by cracking due to fouling, erosion corrosion (due to turbulent flow and suspended solids), and overheating [11]. Titanium alloys of Grades 2 and 5 suffered crevice corrosion in seawater at temperatures of 80 °C and 200 °C, respectively [12]. For titanium of Grade 2, film breakdown/repassivation transients indicated a temperature threshold, around 65 °C, for the initiation of crevice corrosion in 0.27 mol/L NaCl [13]. The authors of [14] noted the initiation of corrosion within one year of operation of a titanium heat exchanger in nitric acid (with a maximum temperature of 107 °C).

Here, we investigated a corrosion failure in a shell and tube type heat exchanger made of titanium (Grade 2) at one of the largest mining enterprises in the world (the Starobin deposit nearby Starobin (Belarus), which is the second-largest processing ore body in the former Soviet Union countries). Belarus accounts for 16% of the global production of potassium [15]. JSC “Belaruskali” gives a fifth of the world’s volume of total potash fertilizers according to data of the International Fertilizers Association [16]. Here, some of the titanium heater tubes inside the heater component were found to fail with severe degradation after less than 5,000 h of operation.

The aim of this study was to investigate this corrosion case of a titanium heat exchanger exposed to KCl-NaCl containing dissolving lye for the processing of sylvinite ore at high temperatures up to 120 °C. This was accomplished by failure analysis and complementary electrochemical measurements at varying temperatures in simulated lye.

## Methodology

*Heat exchanger characteristics*

The heat exchanger (material: titanium VT-1-0 according to GOST 19807, in Germany 3.7034 or Ti2, Grade 2, in England IMI125) is intended for operation in existing heating schemes for dissolving lye (tube space) using saturated water vapor or superheated condensate as a heat carrier. As a result, the lye is heated up to 120 °C under a pressure of 0.6 MPa. The heat exchanger is schematically depicted in Fig. 1. Its total surface area was 179 $m^2$. The orientation of the heat exchanger was horizontal. The shell of the heat exchanger had a temperature disc lens compensator. The pipes were sized 38 mm × 2.0 mm (inner diameter is hence 34 mm) according to VT-1-0 GOST 22897-86. The location of the investigated corrosion is shown in Fig. 1. The location of the corrosion failure was where the

lye reached its maximum temperature before exiting the heat exchanger.

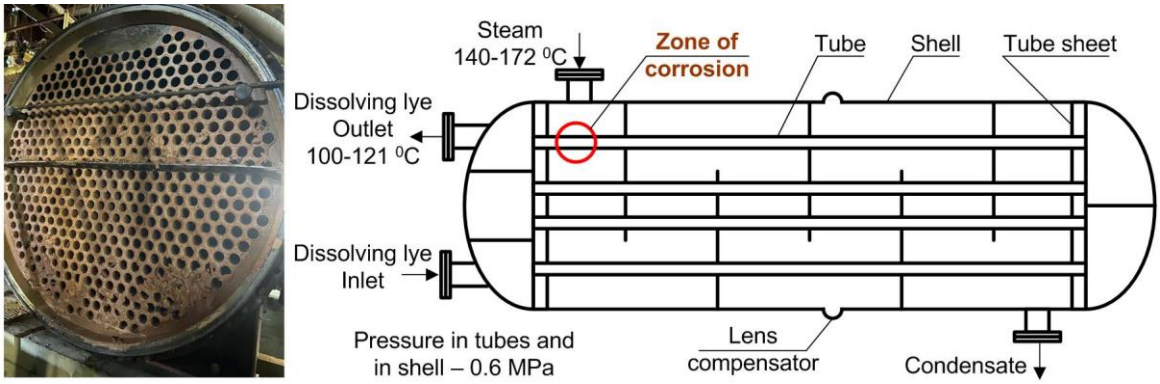


**Fig. 1.** Picture of outlet showing lye deposits (left) and schematic of shell and tube type titanium heat exchanger (right)

The warranty period for the heat exchanger was 24 months from the date of commissioning. The guaranteed service life of the tubes of the tube bundle, excluding the occurrence of corrosion failure in the heat exchanger, was at least 5 years from the moment the apparatus was put into operation.

*Characteristics of the heated dissolving lye*

The flow rate for the pumped lye was 300–600 $m^3$/h in these pipes with an inner diameter of 34 mm. The lye had a density of 1.22–1.24 g/$cm^3$ and a boiling point of 108 °C at atmospheric pressure. The chemical composition of the pumped lye was 9–18 wt.% KCl, 15–19 wt.% NaCl, up to 4.5 wt.% $MgCl_2$ + $CaCl_2$, and 0.1–0.12 wt.% $CaSO_4$, with the remaining part being $H_2O$. The temperature was 60–100 °C (with a maximum of 121 °C), the pH was 6.0–7.5, and the insoluble residue content was up to 150 mg/L. The medium is corrosive, abrasive, and prone to crystallization. For the electrochemical tests, the lower concentration of the indicated concentration range intervals (15 wt.% NaCl, 9 wt.% KCl, 2 wt.% $MgCl_2$, 2 wt% $CaCl_2$, 0.1 wt.% $CaSO_4$, pH 7.08) was used.

*Heating agent characteristics*

The heating agent was water vapor with a working pressure of 0.4–0.6 MPa, at a temperature of 140–172 °C.

*Analysis of bulk composition, surface, and corrosion products*

The surface morphology, elemental composition and elemental distribution of the corrosion products were investigated by means of a JEOLJSM-5610LV scanning electron microscope (SEM) equipped with a chemical micro-X-ray spectroscopic analysis system (EDS) with an accuracy and detection limit of 0.1 wt.%. The magnification was up to 2,000 times. A cross-section was additionally analyzed with a light optical microscope (LOM, an ALTAMI instrument (Russia)).

X-ray diffraction analysis of the obtained samples was carried out on a D8 Advance Bruker AXS X-ray diffractometer (Germany) with the detector being a scintillation counter. The recording was performed in the range of 10–80 degrees (2θ). The obtained X-ray diffraction patterns were identified using the HighScore Plus software and the PDF-2 database.

*Specimen preparation*

For analysis of corrosion products and pits of the corroded areas, specimens were cut from affected areas of the titanium tubes.

For electrochemical investigations, titanium specimens were cut from unaffected locations of the tube, with dimensions of 20 mm × 20 mm. They were then abraded with emery papers down to FEPA P 1200# SiC grit and polished using short synthetic DP-Nap and

diamond pastes (down to 1 µm, DP-Stick P Struers). The specimens were thereafter rinsed with distilled water, degreased by acetone and ethanol (for 5 min each), and dried by nitrogen gas at room temperature (≈ 21 °C). All titanium samples were kept in a desiccator at room temperature for 24±2 h prior to testing to allow a comparable growth of surface oxide.

For cross-sectional analysis (surface morphology, elemental composition and mapping), titanium specimens from affected areas were polished and cleaned, as described for the electrochemical investigations.

*Electrochemical studies*

A Metrohm Autolab PGSTAT 302N potentiostat/galvanostat with three-electrode cells (100 mL), a Ag/AgCl reference electrode in saturated KCl, a Pt grid counter-electrode, and the titanium specimen (exposed area 0.785 $cm^2$) as a working electrode, prepared as described in the section "specimen preparation", were used for the electrochemical measurements (including open circuit potential (OCP), potentiodynamic polarization, and electrochemical impedance spectroscopy (EIS) evaluations). All measurements were performed at room temperature (≈21 °C), 60, 70, 80 and 90 °C and repeated at least two times in the simulated lye solution. The solutions were not deaerated. Electrochemical measurements started with a 1200 s open circuit potential (OCP) scan, followed by electrochemical impedance spectroscopy (EIS) at OCP in the frequency range between 0.01 Hz and 100 kHz at 7 points per decade and a 10 $mV_{rms}$ amplitude. Then, potentiodynamic polarization was run with a scan rate of 1 mV/s from –200 to +1,200 mV relative to the open circuit potential, which was first determined for 20 min.

For statistical analysis of any differences between corrosion parameters extracted from duplicate measurements of potentiodynamic polarization, a Student's *t*-test for unpaired data with unequal variance (KaleidaGraph v. 4.0, Synergy, US) was used. Differences were counted as statistically significant for $P<0.05$. Impedance fitting was performed using the ZView 4 software.

**Results and discussion**

Fig. 2 shows photographs and SEM images of corroded titanium tubes of the heat exchanger used to heat dissolving lye. The photographs (upper two rows in Fig. 2) show millimeter to centimeter-sized holes. The corrosion started from the inside of the tube.

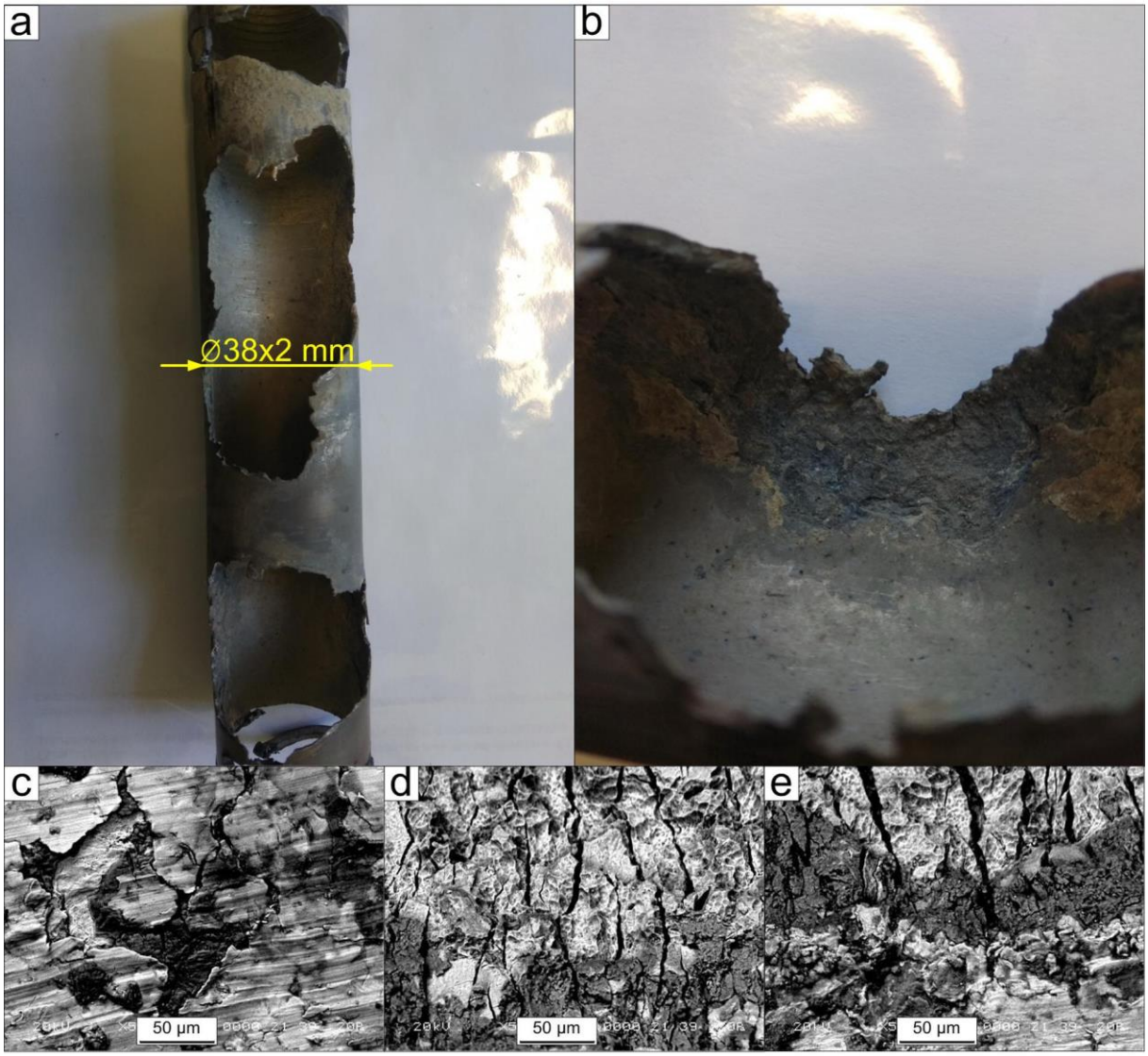


**Fig. 2. Photographs (upper row) and SEM images (lower row) showing millimeter and micrometer-sized cracks and visible corrosion and failure**

The nominal bulk composition of the titanium tube, as provided by the supplier, complied with the composition of titanium Grade 2, Table 1.

**Table 1.** Composition (wt.%) of the investigated titanium tube sample (according to the technical sheet from the supplier) and the standard composition for titanium Grade 2

| Element | Sample | Titanium Grade 2 Standard |
|---|---|---|
| H | 0.0002 | <0.01 |
| O | 0.13 | <0.2 |
| C | 0.006 | <0.07 |
| N | <0.001 | <0.04 |
| Al | 0.017 | Could be <0.7 |
| Si | 0.005 | <0.1 |
| Ti | bulk | 99.2–99.7 |
| Fe | 0.10 | <0.25 |
| Cu+Ni | 0.022 | – |
| Cr+Mn | 0.022 | – |

Based on our previous work [17] in a corrosion failure case for stainless steel, inappropriate cleaning treatments may cause corrosion. However, according to information from the owner of the heat exchanger, the cleaning procedure just included a mechanical descaling.

In order to investigate which substances took part in the extensive corrosion of the titanium tubes, the corrosion products were analyzed. SEM images are presented in Fig. 3 and corresponding EDS results are shown in Table 2.

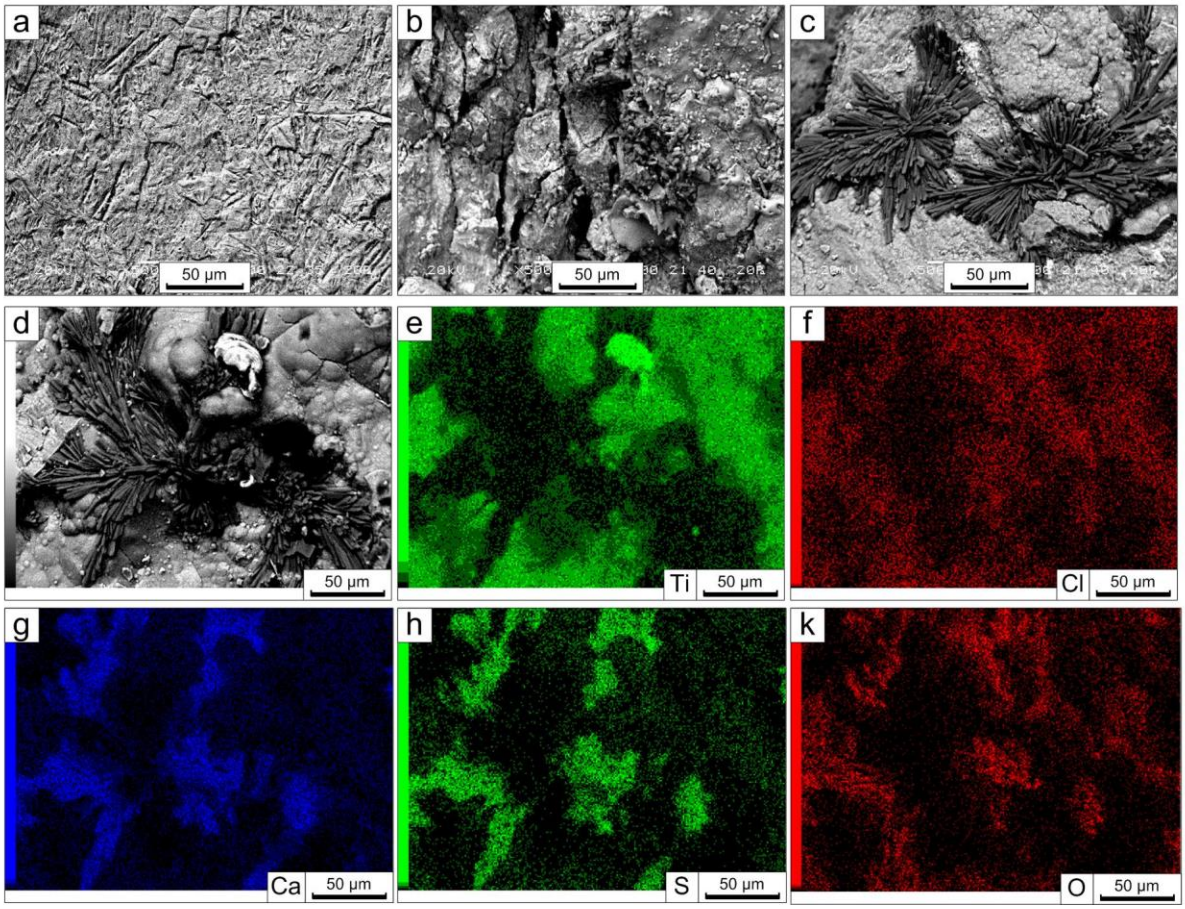


**Fig. 3. SEM images of an unaffected titanium tube (a), corroded area (b), and sediments (c-d) with corresponding (to d) EDS mapping results (e-k)**

The composition of corrosion products, by means of EDS analysis, is shown in Fig. 3 and in Table 2. EDS analysis showed a higher value of Fe for the titanium metal of an unaffected area than did the chemical analysis provided by the supplier (Table 1), suggesting some preferential deposition of Fe impurities from the dissolving lye. Fe, as well as copper (Cu) and zinc (Zn) can catalyze cathodic reactions on titanium metal [18]. Fe, Cu, and Zn are even more enriched in the corroded area (Fig. 3b, Table 2). Deposits (Fig. 3c, Table 2) contain small amounts of these and other impurities, and mainly the dissolving lye main insoluble components (Ca, S, O).

**Table 2**. Composition by means of EDS analysis (average) of corrosion products shown in Fig. 3.

| Element | Fig.3a | | Fig.3b | | Fig.3c | |
|---|---|---|---|---|---|---|
| | wt.% | at.% | wt.% | at.% | wt.% | at.% |
| O | – | – | 26 | 50 | 44 | 66 |
| Al | – | – | 0.33 | 0.38 | 1.0 | 0.89 |
| Si | – | – | 0.43 | 0.48 | 0.51 | 0.43 |
| S | – | – | 1.9 | 1.8 | 12 | 9.1 |
| Cl | – | – | 0.03 | 0.02 | 0.16 | 0.11 |
| Ca | – | – | 5.4 | 4.3 | 27 | 16 |
| Ti | 98 | 99 | 60 | 39 | 12 | 6.2 |
| Fe | 1.6 | 1.3 | 4.3 | 2.4 | 0.27 | 0.12 |
| Cu | – | – | 0.70 | 0.35 | 1.4 | 0.54 |
| Zn | – | – | 1.8 | 0.88 | 0.72 | 0.26 |

Because SEM/EDS only provides measurements from a comparably small area, XRD investigations were also performed for a specimen from a corroded area, with dimensions of 30×30 mm (Fig. 4).

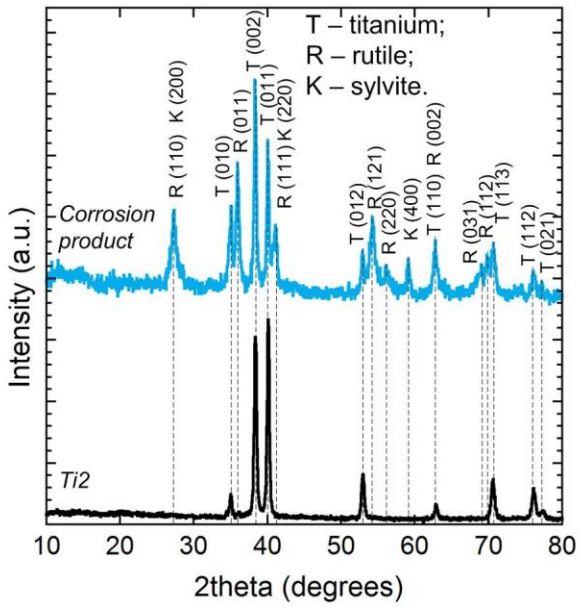


**Fig. 4. XRD diffractograms of corrosion products and bulk titanium (for comparison)**

XRD patterns of the corrosion products showed peaks of titanium metal (hexagonal crystal system and *P63/mmc* space group), rutile (tetragonal crystal system and *P42/mnm* space group) and sylvite (cubic crystal system and *Fm3m* space group), Fig. 4. The main content of the corrosion products was titanium dioxide (rutile). Sylvite was found in the corrosion product samples in a minor concentration and some deposited crystals of calcium sulphate were also found.

To determine whether intergranular corrosion and stress corrosion cracking could have played a role, the cross-section of the corroded specimen was mapped by EDS (Fig. 5). Cracks passed through the titanium oxide and continued into the metal, which is unusual for a corrosion-induced cracking type. Likewise, chlorine was not concentrated at the crack tips or along the cracks. This suggests that the titanium metal could have been embrittled by hydrogen and/or that there were large stresses, facilitating a rapid propagation of the cracks. The distribution of Fe did not imply the participation of Fe (itself) in the corrosion process,

but it could have been a catalyst for the evolution of hydrogen and, therefore, increased hydrogen embrittlement. To conclude, neither intergranular corrosion nor stress corrosion cracking or oxide-induced stress corrosion cracking seemed to be the dominant corrosion propagation mechanism, and a rapid cracking propagation was found. It should be noted that there were no vibrations or other loads during operation of the heat exchanger. There were also no frequent or large temperature variations. When disrupting the processing for maintenance (once every 3 months), only mechanical cleaning and further rinsing with water were used.

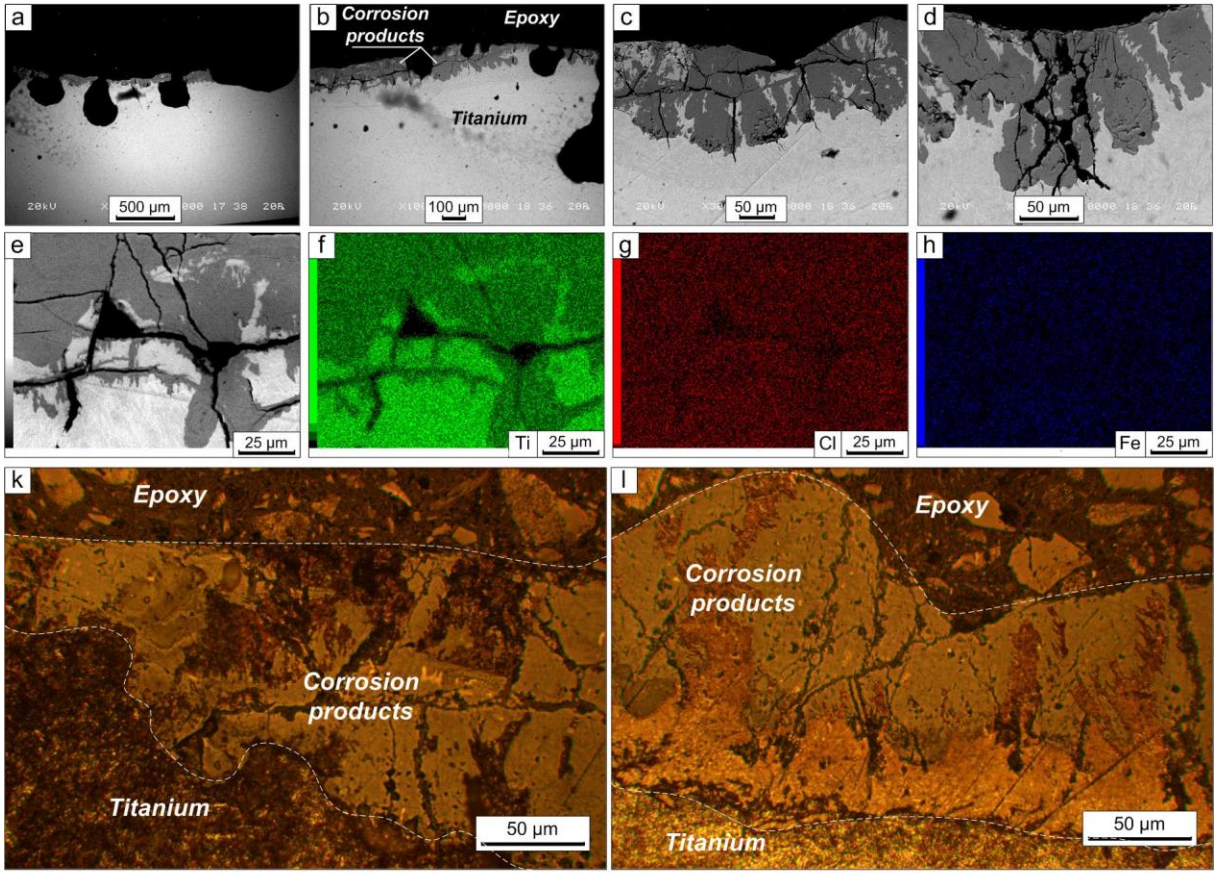


**Fig. 5. Cross-section by SEM (a-d), cross-section and corresponding EDS mapping (e-h), and optical microscope images (k and l)**

For a more complete understanding of the nature of initial corrosion, electrochemical studies were carried out. For these, a simulated dissolving lye solution was used. Representative curves of OCP, PD and EIS are presented in Fig. 6. Corresponding corrosion parameters are presented in Table 3 and Table 4.

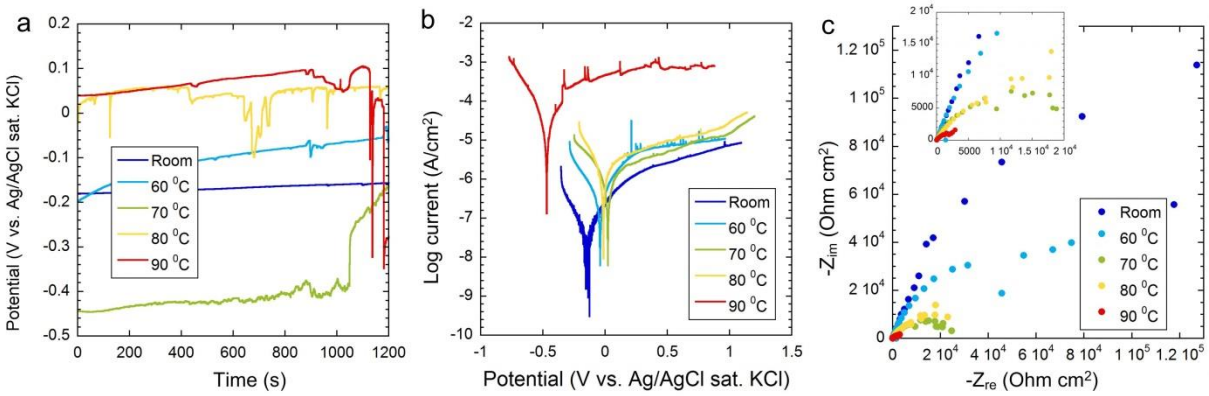


**Fig. 6. Representative curves of OCP (a), potentiodynamic polarization (b) and EIS (c) at room temperature, 60, 70, 80, and 90 °C.**

**Table 3.** Corrosion potential ($E_{corr}$), corrosion current density ($i_{corr}$), anodic branch current density ($i_{ab}$), here defined as the current density at a potential +400 mV *vs.* $E_{corr}$, and pitting potential ($E_{pit}$), respectively. Mean and standard deviations of measurements on two independent samples are shown.

| Temperature, °C | $E_{corr}$, mV | $i_{corr}$, µA/cm$^2$ | $i_{ab}$, µA/cm$^2$ | $E_{pit}$, mV |
|---|---|---|---|---|
| Room | -128±13.0 | 0.0235±0.00345 | 3.85±1.84 | Not reached |
| 60 | -13.1±37.7 | 0.162±0.00367 | 5.05±1.94 | Not reached |
| 70 | 17.9±7.30 | 0.189±0.0302 | 2.91±0.505 | 973±25.5 |
| 80 | -34.8±31.2 | 0.876±0.0520 | 2.34±0.943 | 929±26.2 |
| 90 | -351±167 | 6.967±7.872 | 39.1±37.720 | -25.5±450 |

The corrosion potential (and OCP) first increased slightly with temperature (statistically significant for room temperature compared with 60 and 70 °C) and decreased then (above 80 °C). An increase is probably related to a more rapid oxide growth at higher temperature. The corrosion current was smallest at room temperature and increased with temperature. This was statistically significant for the difference between room temperature and 60 °C. The difference was largest between room temperature and 90 °C (380-fold), while it was a smaller difference for all lower temperatures – with a 20-fold increase between room temperature and 80 °C. Up to 60 °C, there was no pitting breakdown under the tested conditions, while this was the case for the higher temperatures. In order to compare passive and active conditions in this study, we defined an anodic branch current density as the current density 400 mV positive to the corrosion potential (we could not call this a passive current density, since the material was clearly not passivated). This current density increased with temperature, with relatively small differences (statistically significant between 60 and 70 °C) of 4-fold increase from room temperature to 80 °C, while it increased 150-fold from room temperature to 90 °C. The pitting potentials were high and consistent at 70 °C (955 and 991 mV) and at 60 °C (947 and 910 mV) for duplicate samples, while they sharply decreased to 293 and -344 mV at 90 °C.

All these corrosion parameters point towards a serious breakdown of passivity at 90 °C, while there are minor differences up to 80 °C.

**Table 4.** Solution resistance ($R_s$), charge transfer resistance ($R_c$), constant phase element (Q), phase constant element (n), and effective capacitance ($C_{eff}$), as determined from EIS measurements.

| Temperature, °C | $R_s$, Ω cm$^2$ | $R_c$, kΩ cm$^2$ | Q (CPE-T), $\frac{s^n}{(\Omega \cdot cm^2)}$ | n (CPE-P) | $C_{eff}$, μF cm$^{-2}$ |
|---|---|---|---|---|---|
| Room | 5.3±0.2 | 555±85.8 | (8.07±0.034)·10$^{-6}$ | 0.770±0.005 | 0.401±0.016 |
| 60 | 85.2±4.9 | 87.3±0.7 | (54.3±1.66)·10$^{-6}$ | 0.812±0.002 | 15.5±0.095 |
| 70 | 3.8±0.6 | 54.9±52.0 | (43.8±7.64)·10$^{-6}$ | 0.795±0.020 | 4.89±2.53 |
| 80 | 4.2±0.0 | 45.4±4.7 | (44.8±0.065)·10$^{-6}$ | 0.729±0.112 | 5.94±0.05 |
| 90 | 2.3±0.0 | 0.4±0.1 | (222.7±9.82)·10$^{-6}$ | 0.666±0.005 | 4.9±0.066 |

The shape of the Nyquist curve (Fig. 6c) at 90 °C, as compared to the other temperatures, suggests a change from a protective surface oxide to an oxide with possible diffusion.

The strong influence of the temperature above 80 °C suggests that the temperature difference between the corrosion-affected outlet zone (maximum temperature of heat exchanger) and the rest of the titanium tubes of lower temperature might play a role in the rapid corrosion propagation. The relatively small area of higher temperature could have been activated and the relatively large area of lower temperature could have fueled the anodic part-cell corrosion process by providing the surface area necessary for the cathodic reactions. These data are in good agreement with paper [12], which noted crevice corrosion of titanium alloys of Grades 2 at 80 °C in seawater. Another study on titanium of Grade 2 in 0.27 M NaCl found a film breakdown and repassivation transients at a temperature threshold of around 65 °C, initiating crevice corrosion [13].

In all, our investigations suggest that this severe and rapid corrosion failure was mainly caused by the high temperature at the affected area, the temperature difference between affected and non-affected areas, as well as a rapid cracking process, which could have been accelerated by vibrations, pressure-induced stresses, and hydrogen absorption due to the deposition of Fe, Zn, and Cu from the dissolving lye. There were minor temperature variations during operation and no rapid temperature changes, which means that temperature-induced stresses (due to expansion) were probably not part of this corrosion failure. Other facilitating factors were the transported solids resulting in abrasion and difficulties to repassivate, as well as crevices and heat due to deposits. A similar situation was mentioned in [11] where turbulent flow with solids, deposit-induced overheating, and deposit/oxide-induced stresses have been reported as important factors in a corrosion failure of a titanium heat exchanger exposed to hydrocarbon and seawater.

During the maintenance once in three months, the condition of the pipes was checked only visually. In the problem area, this visual inspection should be complemented by non-destructive methods such as ultrasound (to measure the thickness of the pipe), acoustic testing (to distinguish brittle from ductile metal and detect cracking), and electrochemical measurements (to detect the onset of active corrosion by a lower than usual potential). Further, frequent removal of corrosion products from process streams is essential to avoid the formation of crevices and thick deposits that cause overheating. Such Fe-containing deposits may lead to a greater hydrogen evolution and a greater extent of cathodic reactions [4], resulting in greater hydrogen-induced cracking. Surface modification of titanium tubes by pickling, passivation and thermal oxidation can be considered to minimize corrosion attack and hydrogen-induced cracking [7, 14].

## Conclusion

This study presented a corrosion failure of a titanium (Grade 2) heat exchanger used to process dissolving lye (to process sylvinite ore) with high salt content and suspended solids under a flow and pressure and a temperature of up to 121 °C. At the dissolving lye outlet, the location of highest temperature, the tube corroded rapidly within 5,000 h of operation, through rapid cracking starting from the inside of the pipes. EDS analysis suggested a preferential deposition of Fe from the dissolving lye on the titanium surface, which could result in increased hydrogen evolution. Affected corroded areas showed a rapid cracking process progressing through both oxide and metal and not dominated by intergranular corrosion or stress-corrosion cracking. This suggests the involvement of hydrogen embrittlement and external stresses. Electrochemical measurements showed a clear onset of active corrosion above a temperature of 80 °C, suggesting that the high temperature and the temperature difference to the remaining surface of the heat exchanger could have played a major role. The flow with suspended solids and the high extent of deposits causing crevices and possibly overheating could have been participating factors. Non-destructive testing of the most heated area, more frequent cleaning, and a protection against abrasive solids are suggested measures to prolong service life in future.

## Acknowledgements

The authors gratefully acknowledge the financial support of the Ministry of Science and Higher Education of the Russian Federation in the framework of Increase Competitiveness Program of NUST «MISiS» (grant number K2-2020-024), implemented by a governmental decree dated 16th of March 2013. N 211; Wolfe-Western fellowship [grant number: 2020]; Canada Research Chairs Program [grant number 950 – 233099].

## References

1 Boyer, R., Welsch, G., Collings, E.W. (1994). Materials properties handbook: titanium alloys. Materials Park (OH): ASM International.

2 Santos, I.G.R., Vacchi, G.S., Silva, R., Kugelmeier, C.L., Magalhães, D.C.C., Campesan, G. R., Rovere, C. A. D. (2020). Failure analysis of a titanium Coriolis mass flow meter: A case of hydrogen embrittlement. *Engineering Failure Analysis*, *115*, 104618. https://doi.org/10.1016/j.engfailanal.2020.104618

3 Covington, L.C. (1979). The influence of surface condition and environment on the hydriding of titanium. *Corrosion*, *35*(8), 378-382.

4 Covington, L., Schutz, R. (1981). Effects of Iron on the Corrosion Resistance of Titanium. Industrial Applications of Titanium and Zirconium, ed. E. Kleefisch (West Conshohocken, PA: ASTM International, 163-180. https://doi.org/10.1520/STP28066S

5 Chen, F.J., Yao, C., Yang, Z.G. (2014). Failure analysis on abnormal wall thinning of heat-transfer titanium tubes of condensers in nuclear power plant Part I: Corrosion and wear. *Engineering Failure Analysis*, *37*, 29-41. http://dx.doi.org/10.1016/j.engfailanal.2013.11.003

6 Chen, F.J., Yao, C., Yang, Z.G. (2014). Failure analysis on abnormal wall thinning of heat-transfer titanium tubes of condensers in nuclear power plant Part II: Erosion and cavitation corrosion. *Engineering Failure Analysis*, *37*, 42-52. https://doi.org/10.1016/j.engfailanal.2013.11.002

7 Yang, Z.G., Gong, Y., Yuan, J.Z. (2012). Failure analysis of leakage on titanium tubes within heat exchangers in a nuclear power plant. Part I: Electrochemical corrosion. *Materials and Corrosion*, *63*(1), 7-17. https://doi.org/10.1002/maco.201106189

8 Gong, Y., Yang, Z.G., Yuan, J.Z. (2012). Failure analysis of leakage on titanium tubes within heat exchangers in a nuclear power plant. Part II: Mechanical degradation.

*Materials and Corrosion*, *63*(1), 18-28. https://doi.org/10.1002/maco.201106190

9 Shen, S., Li, X., Zhang, P., Nan, Y., Song, X. (2016). Failure Analysis and Fatigue Investigation on Titanium Tubes in a Condenser. *Journal of Failure Analysis and Prevention*, *16*(6), 975-981. https://doi.org/10.1007/s11668-016-0171-5

10 Ma, Q.L., Xu, H., Wang, Z.W., Hou, F., Xu, L.Y. (2005). Failure analysis and critical manufacturing technology research on titanium condensers. *Engineering Failure Analysis*, *12*(3), 432-439. https://doi.org/10.1016/j.engfailanal.2004.10.005

11 Shalaby, H.M., Al-Mazeedi, H., Gopal, H., Tanoli, N. (2011). Failure of titanium condenser tube. *Engineering Failure Analysis*, *18*(8), 1990-1997. https://doi.org/10.1016/j.engfailanal.2011.05.008

12 Pang, J., Blackwood, D.J. (2016). Corrosion of titanium alloys in high temperature near anaerobic seawater. *Corrosion Science*, *105*, 17-24. http://dx.doi.org/10.1016/j.corsci.2015.12.011

13 He, X., Noël, J.J., Shoesmith, D.W. (2002). Temperature dependence of crevice corrosion initiation on titanium grade-2. *Journal of the Electrochemical Society*, *149*(9), B440. https://doi.org/10.1149/1.1499501

14 Shankar, A.R., Sole, R., Thyagarajan, K., George, R.P., Mudali, U.K. (2019). Failure analysis of titanium heater tubes and stainless steel heat exchanger weld joints in nitric acid loop. *Engineering Failure Analysis*, *99*, 248-262. https://doi.org/10.1016/j.engfailanal.2019.02.016

15 Roberts, T.L. (2008) Global Potassium Reserves and Potassium Fertilizer Use http://www.ipni.net/ipniweb/portal.nsf/0/9c5cff1af71db2ce852574e8004ecc00/%24FILE/Roberts%20-%20ASA%20Nutrient%20Cycling%20Symposium%20Potash.pdf

16 https://kali.by/en/

17 Romanovski, V., Frantskevich, V., Kazlouski, V., Kasach, A., Paspelau, A., Hedberg, Y., Romanovskaia, E. (2020). Inappropriate cleaning treatments of stainless steel AISI 316L caused a corrosion failure of a liquid transporter truck. *Engineering Failure Analysis*, *117*, 104938. https://doi.org/10.1016/j.engfailanal.2020.104938

18 Noel, J.J. (1999). The electrochemistry of titanium corrosion. University of Manitoba, Winnipeg, Manitoba.